We are IntechOpen, the world's leading publisher of Open Access books Built by scientists, for scientists

4,800
Open access books available

122,000
International authors and editors

135M
Downloads

Our authors are among the

154
Countries delivered to

TOP 1%
most cited scientists

12.2%
Contributors from top 500 universities

CLARIVATE ANALYTICS BOOK CITATION INDEX INDEXED

WEB OF SCIENCE™

Selection of our books indexed in the Book Citation Index in Web of Science™ Core Collection (BKCI)

Interested in publishing with us?
Contact book.department@intechopen.com

Numbers displayed above are based on latest data collected.
For more information visit www.intechopen.com

Chapter

Artificial Intelligence in Light-Source Design

Snjezana Soltic and Andrew N. Chalmers

Abstract

The advent of light-emitting diode (LED) light sources has led to a new freedom in the design of light-source spectra, and it is now possible to optimise for different source performance parameters, which is the principal aim of the authors' work. LEDs and lasers are real or potential light sources, and are inherently monochromatic, that is, narrow-band sources, with typical optical bandwidths in the range 20–40 nm (nanometres) for LEDs and 1–5 nm for diode lasers. Mixtures of three or more can be used to produce nominally white light of the type acceptable for general purpose lighting. It is a characteristic of all types of sources that there is a trade-off between good colour properties and high efficiencies, and the methods described here are directed towards an optimum combination of such parameters. This chapter will explain the use of differential evolution (DE) as a highly effective heuristic approach to optimisation, and proceeds to explain the structure and operation of a DE algorithm designed as an optimisation tool for such purposes.

Keywords: differential evolution, optimisation, LED lighting, luminous efficacy, correlated colour temperature, colour rendering and fidelity

1. Introduction

It has been stated by some authors that white LEDs are the eco-friendly light sources for the twenty-first century [1]. White light in LEDs can be produced either (i) by using blue (or violet) light to irradiate a phosphor that emits yellow light [2, 3] or (ii) by combining the outputs of a group of monochromatic LEDs [1, 4, 5]. In approach (i) the blue or violet is combined with the yellow to produce white light. We have adopted approach (ii) in which three (or, preferably, four) primary colours are mixed in appropriate proportions to produce high-quality white light with higher efficiency than approach (i) since there is no loss of energy as in the down-conversion in the phosphor [5, 6]. Both approaches aim to design LED-based white-light sources characterised by high colour rendering and fidelity properties combined with high luminous efficacy. It is an established fact in light-source design that these two qualities are generally contravariant, and that both depend on the emitted spectrum of the source. We have found that fine-tuning of the intensities of the individual sources, as well as the selection of their individual peak wavelengths, enables us to define the best balance of the significant spectral properties of the mixture. Our adopted optimisation technique implements a trial-and-error search algorithm within an n-dimensional space $\{I_1, \ldots, I_i, \ldots, I_n\}$ until an acceptable spectral power distribution (SPD) is found for the white-light mixture [5, 7, 8].

In this chapter, we will describe an approach to the design of the optimum LED mixture using a simple global optimisation algorithm based on differential evolution (DE) as proposed by Storn and Price [9]. We have optimised the SPDs of mixtures of real and simulated LEDs and diode lasers. For this purpose, a MATLAB program was developed that optimises the SPD of an arbitrary mixture of individual SPDs. Specific versions of this program were developed to implement several different techniques for defining (and calculating) the colour properties of sources.

This chapter proceeds as follows. In Section 2, the principles of the DE algorithm are described in detail. In Section 3, the theory of colour rendering and luminous efficacy is given, along with other relevant lighting terms and their usage. Section 4 presents a selection of key experimental results and comparisons and, finally, we state our conclusions in Section 5.

2. Differential evolution

Differential evolution is a powerful population-based evolutionary algorithm suitable for the optimisation of real-value multi-modal non-linear and non-differentiable objective functions $f_o(x_1, x_2, \ldots, x_n)$ [9, 10]. DE is simple and has proven to be powerful in solving a number of benchmark problems [11, 12].

The search for an optimal solution starts with a population of P randomly created solution vectors $\{v_1, v_2, \ldots, v_P\}$. This population is maintained constant during the optimisation process, during which the solution vectors (i.e., candidate SPDs) undergo mutation, crossover, evaluation and selection over a number of generations G. The best choices for both the population size P and the number of generations G depend on the problem to be optimised. Storn and Price suggest $P \in [5n, 10n]$, where n is the dimension of the objective function, but P must be ≥ 4 to provide sufficient mutually different solution vectors for the algorithm to function properly [10].

The operation of the algorithm is controlled by the use of a fitness function f_{fit} designed to discriminate between solutions (SPDs here) with 'good' or 'poor' properties.

Mutation is the process of creating a new offspring vector $u_{i,G+1}$ by adding the weighted difference between two randomly chosen solution vectors, $v_{r2,G}$ and $v_{r3,G}$, to a randomly chosen $v_{r1,G}$ [10]:

$$u_{i,G+1} = v_{r1,G} + F \times (v_{r2,G} - v_{r3,G}) \tag{1}$$

where F is a mutation weight $\in [0,2]$ and random indices $r_1, r_2, r_3 \in [0, P-1]$ are chosen to be different from the index i. The mutation process is illustrated in **Figure 1**.

The offspring solution vectors $u_{i,G+1}$ undergo crossover which ensures that the offspring vectors $w_{ji,G+1}$ differ from their parents [10]:

$$w_{ji,G+1} = \begin{cases} u_{ji,G+1} & \text{if } (j \leq CR) \mid (j = i) \\ v_{ji,G} & \text{if } (j > CR) \mid (j \neq i) \end{cases} \tag{2}$$

where the terms and parameters are defined as follows: $i \in \{1,2,\ldots, P\}$ is a randomly chosen integer, $j \in [0, 1)$ is a randomly chosen real value, $CR \in [0, 1]$ is a crossover constant influencing the number of elements to be exchanged. An example of the crossover process is shown in **Figure 2**.

The process compares the offspring vectors $\{w_{1,G+1},\ldots, w_{P,G+1}\}$ against their parent vectors $\{v_{1,G},\ldots, v_{P,G}\}$. If the offspring $w_{i,G+1}$ has a better fitness function f_{fit} than its parent $v_{i,G}$, then it becomes a member of the next generation, $G + 1$. If not,

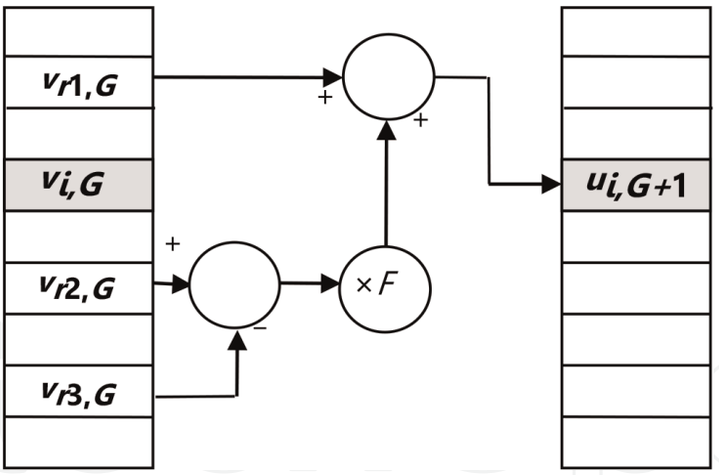

Figure 1.
Illustration of the mutation process for P = 9.

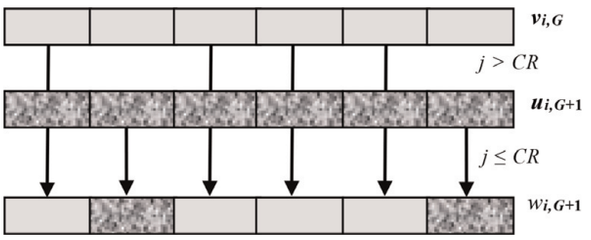

Figure 2.
Illustration of a typical crossover process for P = 6.

the $v_{i,G}$ vector is retained. Hence, only the fitter offspring become members of the $G + 1$ generation.

Proposals have been made for several variants of the original DE algorithm [10]. The most significant differences are in the creation of new solution vectors where:

1. the best solution vector from the current generation $v_{best,G}$ is mutated rather than $v_{r1,G}$;

2. more than two difference vectors are used in mutation; and

3. different crossover schemes are employed.

Our work is based on the original DE, and is described in pseudo-code given below:

Require: G, P, F ∈[0,2], CR ∈[0,1]
1: Create vectors $\{v_{1,0},\ldots,v_{P,0}\}$
2: Evaluate $\{v_{1,0},\ldots,v_{P,0}\}$->$f_{fit,0}$
3: for all G do
4: Mutate $v_{i,G}$ -> $u_{i,G+1}$
5: Crossover $\{u_{1,G+1},\ldots,u_{P,G+1}\}$ and $\{v_{1,G},\ldots,v_{P,G}\}$->$\{w_{1,G+1},\ldots,w_{P,G+1}\}$
6: Evaluate $\{w_{1,G+1},\ldots,w_{P,G+1}\}$
7: if $f_{fit}(w_{i,G+1}) > f_{fit}(v_{i,G})$
8: $v_{i,G+1} = w_{i,G+1}$
9: else
10: $v_{i,G+1} = v_{i,G}$
11: end if
12: end for

3. Light-source properties

Our purpose in this chapter is to present an approach to intelligent spectral design for any white-light source, aiming to achieve an optimum combination of luminous efficacy and colour rendering which, as previously noted, are contravariant characteristics of the SPD. We next introduce a brief outline of these, and other important, source properties.

3.1 Colour rendering index

Colour rendering has been defined by the *Commission Internationale de l'Éclairage*, International Commission on Illumination (CIE) who have published recommendations for the method of calculation of their colour rendering index (CRI) [13] based on a knowledge of the light-source spectrum. It represents an evaluation of the average colour shift of eight defined moderate-chroma colour samples when compared under the test source and a reference source having the same correlated colour temperature (CCT).[1] The system includes 14 test colours in total, and the additional 6 comprise 4 highly saturated colours (red, yellow, green, and blue) plus samples representing skin and foliage colours, respectively. As of the time of writing, this is the internationally agreed method. Note that CRI and associated technology have also been covered in [14]. The two most widely quoted colour rendering terms are: R_a—the general colour rendering index, based on the colour shifts of the eight principal test colour samples; and R_9—the 'special' (individual) index for the highly saturated red colour (sample 9).

In our optimisation work (see Section 4.1), we also made use of several derived indices symbolised as R_b, R_c and R_{min}, based, respectively, on: the 6 additional test colours; the full set of 14 test colours and the minimum individual value from the R_c set.

3.2 Colour fidelity index

Some dissatisfaction with the CIE method has arisen since the widespread adoption of LED lighting. As a consequence, the Illumination Engineering Society of North America (IES) has adopted a recommended method (TM-30-15) [15, 16] which recommends two new indices (R_f and R_g) for the classification of the colour properties of light sources. The underpinning research leading to the development of TM-30-15 [16–18] identified several weaknesses in the CIE's earlier CRI method [13], claiming that it does not adequately sample wavelength space and hence tends to over-estimate colour performance.

The method is also based on the colour-shift concept, but now using a set of 99 test colours considered to provide uniformity of both wavelength sampling and colour-space sampling. In addition, it uses a more modern colour-difference calculation technique, CAM02UCS [19] which is a development of the basic CIECAM02 colour appearance space [20].

The new index R_f gives an overall assessment of colour fidelity, while gamut index R_g indicates the relative magnitudes of colour shifts for sample colours in different regions of colour space. Also available is the skin colour index, $R_{f\,skin}$, which is an average of two specific sample-colour indices, selected as representative of human skin. In our optimisations, we also called up the minimum value of R_f,

[1] Defined in Section 3.5.

symbolised as $R_{f\,min}$, from the full set of 99 individual indices $R_{f\,i}$, as well as the referenced colour sample number i_{min} (in the set i_1 to i_{99}).

3.3 Colour quality scale

This was a precursor to TM-30-15, first proposed by Davis and Ohno of NIST (USA) [21]. The following serves as a brief introduction for the purpose of the present discussion. Again using the previously mentioned colour-shift concept, the CQS metric employs 15 saturated test colour samples, on the premise that certain light sources may render saturated colours more poorly than the de-saturated colours of the CIE's CRI method. The chromatic differences are calculated using the CIE 1976 (CIELAB) colour model [22].

The full calculation procedure has also been explained in [23]. It employs multiple steps, several of which are non-linear, resulting in the general CQS index, Q_a. As with the previous two cases, the 'special CQS' (Q_i) for each test colour sample may be calculated for a more thorough investigation of a test source. We have used the minimum value of Q_i (designated Q_{min}) from the set of 15 Q_i values, as an optimisation parameter.

3.4 Luminous efficacy of radiation

The luminous efficacy of the radiation (LER) of a light source assesses the 'lighting content' of the spectrum by comparing the visible light output (in lumens) to the total radiant output (in watts) as in Eq. 3.

$$LER = \frac{K_m \int_\lambda V(\lambda) S(\lambda) d\lambda}{\int_\lambda S(\lambda) d\lambda} \tag{3}$$

where K_m is the maximum luminous efficacy of radiation (≈683 lumen per watt), $S(\lambda)$ is the spectral distribution of the light source, and $V(\lambda)$ is the CIE spectral sensitivity function for human photopic vision [24]. The LER is an important determinant of the overall economy of a light source since the overall luminous efficacy is given by the product of LER with the energy conversion efficiency of the particular light source.

3.5 Correlated colour temperature

From the perspective of the lighting system designer, the correlated colour temperature (CCT) is the key feature in the selection of a light source since the CCT serves as an indicator of, not only the colour of the source, but also, the 'atmosphere' it will create.

The CCT is defined in [25], and its significance is that it describes the chromaticity of the source (which must be close to the Planckian locus) in the CIE (u, v) chromaticity diagram.[2] Note that it is possible for many different spectral power distributions (SPDs) to have the same CCT; and that CCT is not essentially linked with colour rendering, quality or fidelity.

[2] In CIE documentation, this is now replaced by the $\left(u', \frac{2}{3}v'\right)$ diagram based on CIE 1976 (u', v') coordinates.

4. Optimisations

We here present, in outline form, the results of optimised spectral designs achieved using DE. Interested readers are referred to previous publications [23, 26–29] for full details.

It is noted at the outset that it is, in principle, possible to create white-light mixtures by the use of as few as two or three wavelengths. Our early experiments showed that these practically always lead to suboptimal mixtures in the sense that either one or both of LER and X_c are unacceptably low (X_c is here used to denote any one of the colour metrics mentioned in Section 3). Further experiments indicated that mixtures of five, six or seven wavelengths gave little or no practical advantage over 4-band mixtures, while adding to the complexity (and possible unreliability) of the light source. For the sake of brevity, therefore, the following descriptions are confined solely to results for 4-band mixing.

Two types of optimisation conditions are described: (i) constrained, in which the optimiser is presented with a set of known (e.g., commercial) monochromatic spectra, and is required to find the best available mixtures in terms of defined criteria and (ii) unconstrained, when the program is given mathematical descriptions for the shapes of potential monochromatic spectra, which it then proceeds to mix and optimise as above.

In the optimisations described below, all SPDs for LEDs were computed at 5-nm intervals, and for lasers at 1 nm.

4.1 Optimisation of LED mixtures for LER and CRI (CIE R_a)

This investigation [26] explored the optimisation of white-light mixtures of seven LEDs (four at a time) from the Lumileds Luxeon™ range [30] and it is therefore classed as constrained. The objective here was to achieve the best available combination of R_a with LER, and the fitness function for DE was defined as in Eq. 4:

$$f_{fit} = aR_a + bR_b + cR_c + d_{rad} + eR_{min} \tag{4}$$

where R_a = CIE general colour rendering index (based on 8 medium-chroma test colours); R_b = similar figure of merit based on the 6 additional test colours in the CIE method; R_c = similar figure of merit based on all 14 test colours in the CIE method; η_{rad} = the value of the LER (lumen per watt figure); R_{min} = the lowest value of R_i in the set of 14 individual values; a, b, c, d and e are user-selectable weights controlling the influence of R_a, R_b, R_c, η_{rad} and R_{min} on the optimisation process.

Experimentation found that f_{fit} converged around (or before) the 1000th generation; hence, the number of generations G was set to 1000 for fast and accurate convergence of the DE. Note that a too-small G can mean that the process has insufficient opportunity to search for effective solution vectors whereas, for excessive values of G, the optimisation process is unnecessarily slowed down without improving the optimisation result.

The other DE parameters that may influence the operation of the algorithm are P, F, and CR, all of which need to be set prior to any run. We found by experimentation that the values of these parameters had only a minor influence on the optimisation results; and the choice of suitable values for good optimisation was straightforward. We quickly settled on a value of P = 50, and we set F and CR according to the suggestions in [10], that is, F = 0.5 and CR = 0.1.

Further experimentation investigated the effects of different values for the weighting factors for f_{fit}, and some indicative results are shown in **Table 1**. The relative spectral power distribution (SPD) for the result listed as Test 1 is shown in **Figure 3**.

Test no	Weighting factors					Best results						
	a	b	c	d	e	R_a	R_b	R_c	η_{rad} (lm/W)	R_{min}	i_{min}	CCT (K)
1	1	1	1	1	10	95	96	91	339	76	12	3268
2	1	1	1	1	5	93	83	89	350	76	12	3074
3	1	1	1	0.5	0	92	79	87	384	58	9	3169

Table 1.
Influence of different f_{fit} weights on the optimization of LED mixtures.

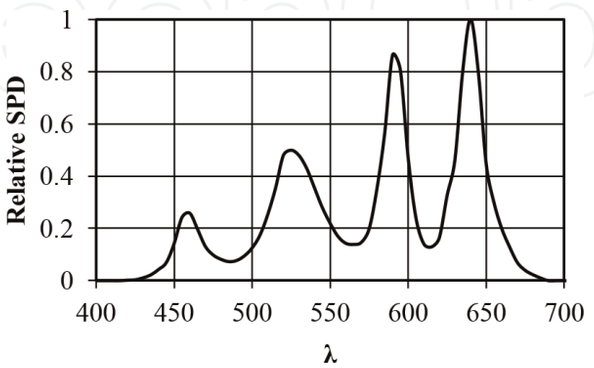

Figure 3.
Relative SPD of the 4-band LED mixture (Test 1). Wavelength peaks for: blue = 460 nm, green = 530 nm, amber = 590 nm, red = 630 nm. Source parameters: R_a = 95, R_b = 86, η_{rad} = 339 lm/W, CCT = 3268 K, R_{12} = 76 (blue sample).

It is worth noting that $R_a \geq 90$ is generally considered as excellent colour performance, and LER ≥ 300 lm/W exceeds that of many other (efficient) light sources.

Table 1 shows that significant step decrements in the weight e (the R_{min} weighting) led to fairly small losses in the colour performance of the mixtures, but to noticeable gains in LER (and hence, efficiency in use).

Figures 4 and **5** show how the individual elements of f_{fit} in Test 1 were fluctuating before converging to their final values.

It can be seen that η_{rad} (**Figure 5**), and hence also f_{fit}, undergoes significant swings during the early stages of the process ($G < 300$). It then converges to just below 340 lm/W at G = 336. In this instance, the population has converged around G = 400, and all parameters are only fine-tuned thereafter. These curves indicate that the process could, in fact, have been terminated at G = 500, with low likelihood of loss.

4.2 Optimisation of mathematical mixtures for LER and CRI (CIE R_a)

It was decided to extend the above approach to an unconstrained investigation of SPD mixtures defined by the following mathematical functions:

- Gaussian
- rectangular
- triangular

The optimiser was free to position four spectral bands, conforming to any one function, at any wavelength within the visible band (380–760 nm) and having any relative intensity (i.e., height) of one to another. One constraint was imposed for practical purposes, namely each band was kept to a spectral width between 25 and

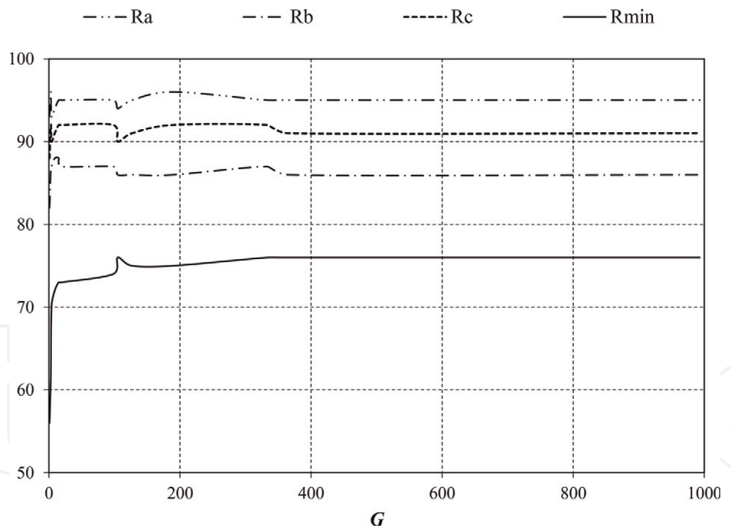

Figure 4.
Behaviour of R_a, R_b, R_c and R_{min} in Test 1.

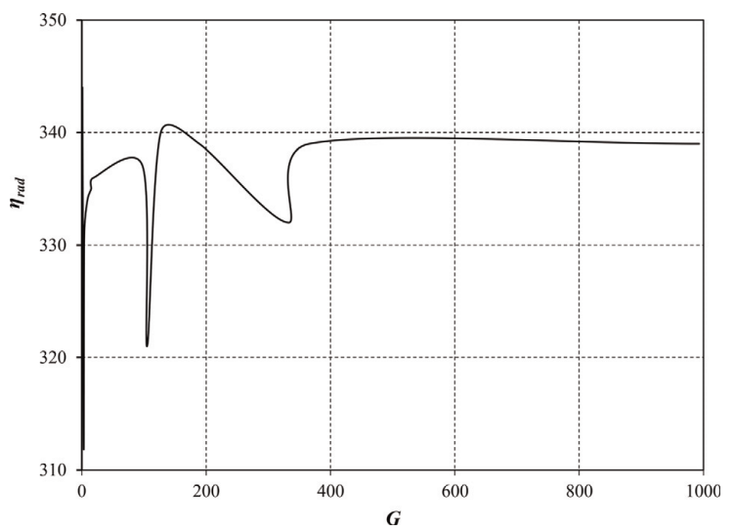

Figure 5.
Behaviour of η_{rad} in Test 1.

45 nm (full width at half maximum, or FWHM) [27]. Apart from these changes, the procedure was essentially the same as that used in Section 4.1, and the same fitness function was used.

A total of 36 optimisations were performed, using 12 different combinations of f_{fit} weightings for each of the three functions. The following extract from this set of results shows the SPDs obtained with the weightings: $a = 1$; $b = c = d = e = 0$. See **Figure 6**.

It was intended that the unconstrained approach will help to identify those wavelength combinations that will lead to optimum SPDs. The findings relating to the spectra in **Figure 6** are summarised in **Table 2**.

This is too small a sample from which to generalise; however, it is possible to make the following observations. The colour performance of these three mixtures is exceptionally good (other than the high CCT for G1) possibly at the expense of relatively moderate LER values. It is probable that the Gaussian and triangular shapes are more realistic simulations of real physical spectra (whether originating from LEDs or phosphors); hence their corresponding centre wavelengths (λ_1–λ_4) may be useful indicators for use in light-source design. See [27] for a more complete discussion.

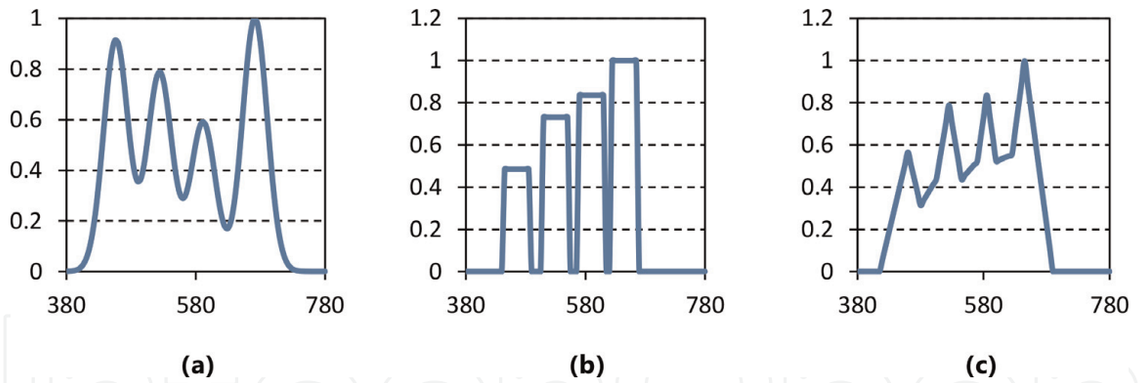

Figure 6.
Relative SPDs of the mathematical 4-band mixtures. (a) G1, Gaussian; (b) R1, rectangular; (c) T1, triangular $f_{fit} = R_a$.

Expt	R_a	R_b	R_c	η_R (lm/W)	R_{min}	i_{min}	T_C (K)	λ_1	λ_2	λ_3	λ_4
G1	98	93	96	228	80	12	7870	456	524	591	671
R1	97	90	94	317	72	12	3542	445	510	570	625
T1	98	95	97	303	84	12	4133	460	525	585	645

Table 2.
Results for the mixtures of mathematical functions shown in ***Figure 4****.*

4.3 Optimisation of LED mixtures for LER and CQS (NIST Q_a)

This was again a constrained optimisation process. It was based on the same set of Luxeon™ LEDs as used in Section 4.1, and also used tetrachromatic mixtures. The optimisation process [23] was also broadly similar to that in Section 4.1, and it used a similar interface, but the software was rewritten to compute the performance of candidate SPDs in terms of CQS parameters, specifically the average colour quality index, Q_a, and the minimum, Q_{min} (the lowest individual index, Q_i) for every candidate SPD.

The following fitness function (Eq. 5) was employed:

$$f_{fit} = aQ_a + b\eta_{rad} + cQ_{min} \tag{5}$$

where a, b, c are the weights controlling the influence of Q_a, LER and Q_{min} on the optimisation of the LED mixtures. A selection of the results of the optimisation of the LED mixtures using various weightings is shown in **Table 3**.

Weights			Optimised spectra			
a	b	c	Q_a	η_{rad} (lm/W)	Q_{min}	CCT (K)
1	0	0	96	306	93	3638
1	0	1	96	305	94	3386
0	0	1	96	298	94	3379
10	1	0	95	322	91	3452
0	1	2	84	367	75	5041

Table 3.
Optimizations of five tetrachromatic LED mixtures (CQS domain).

4.4 Optimisation of LED mixtures for specific CCT values

The previously mentioned techniques (used in Section 4.1–4.3) did not take account of the CCTs of the spectra except as values to be calculated following the optimisations. Because of the importance of the CCT to lighting designers and users, it was recognised that this parameter needed to be incorporated into the optimisation procedure.

We therefore designed a new optimisation tool [29], again based on differential evolution, which puts CCT at the centre of the process and then proceeds to optimise colour rendering while maintaining a close tolerance to the target CCT value. We selected three CCT values to illustrate the effectiveness of the process.

The optimiser was presented with a specific set of four monochromatic LED spectra selected from the Luxeon™ range. The objective was to minimise the average colour difference for a set of colour samples which, in principle, could be any suitable set of colours. We chose to use the 14 test colours specified in CIE13.3 [13] since they constitute a well-known and widely used set.

The basis of the selection process in our algorithm was the colour difference of specific surface colours as they appear under the candidate spectrum and under the reference spectrum of the same CCT. In each new generation, the offspring solutions were evaluated on the basis of minimising the colour difference $\Delta E_{00(Avg)}$ calculated using the CIEDE2000 colour difference formula [31]. Hence, the algorithm was designed to search for a spectrum with the lowest colour differences. The optimum solution was determined after having performed G generations (typically 1000); that is, the best solution in generation G is accepted as the best white-light spectrum.

Figure 7 shows the results in the form of the SPDs realised by the LED mixtures, and their performance is summarised in **Table 4**. Note that $\Delta E_{00(Avg)}$ represents the average of 14 colour differences (for the 14 colours in the CIE set) and $\Delta(u',v')$ is the chromaticity difference in CIE 1976 coordinates between the target CCT and that achieved by the LED mixture. The other listed parameters were computed after the completion of each optimisation run.

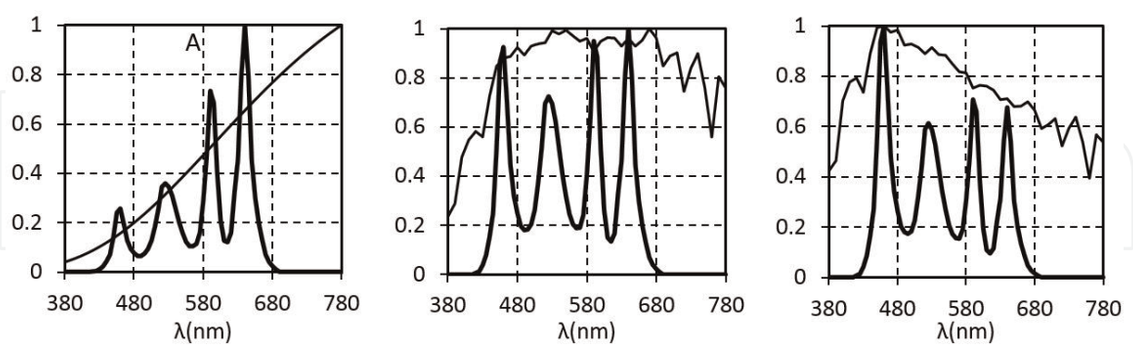

Figure 7.
Relative SPDs of 4-LED mixtures that match CIE illuminants A, D50 and D65. Relative SPDs of the actual illuminants are shown for reference (lighter lines).

Illuminant	R_a	R_{min}	i_{min}	LER (lm/W)	$\Delta E_{00(Avg)}$	$\Delta(u',v')$
A	93	68	11	313	0.73	0.0038
D50	95	70	12	311	0.81	0.0010
D65	95	63	12	298	0.94	0.0015

Table 4.
Optimizations of tetrachromatic LED mixtures with specified CCTs.

Illuminant	R_a	R_{min}	i_{min}	LER (lm/W)	$\Delta E_{00(Avg)}$	$\Delta(u',v')$
A	96	68	12	318	0.82	0.0034
D50	95	89	12	336	0.58	0.0019
D65	93	75	9	299	0.67	0.0059

Table 5.
Optimizations of tetrachromatic Gaussian mixtures with specified CCTs.

The above approach was extended to a set of optimisations in which Gaussian-shaped spectra of either 25 or 50 nm bandwidth, but with unconstrained peak intensities and wavelengths, were optimised in the same way as the LED mixtures.

Table 5 shows the best CRI performance for 4-band (25 nm) Gaussian mixtures, along with the other properties as listed in **Table 4**, and there is an evident degree of conformance between the two sets of results.

4.5 Optimisation of laser diode mixtures using TM-30-15 (IES R_f)

Our investigations in this field [28, 32] were inspired by the work of Neumann et al. [33] who successfully demonstrated a white-light 4-laser mixture with acceptable colour properties expressed in terms of the CRI and CQS metrics. Our earlier paper [28] also used CRI and CQS as measures of colour rendition. These approaches are now regarded as suspect (particularly in respect of mixtures of ultra-narrow bands such as lasers) on the grounds of incomplete sampling of wavelength and colour spaces.

Our purpose in [32] was to optimise similar mixtures of solid-state lasers, and to utilize the more up-to-date method of the IES colour fidelity index R_f [15, 16].

A new optimisation tool was designed to implement the complex sequence of non-linear calculation steps in the evaluation of colour fidelity for any given SPD. We then developed a new fitness function (Eq. 6) based on the IES parameters as well as the LER, to evaluate every candidate spectrum produced in the process.

$$f = aR_f + bR_{f\ \mathrm{min}} + cR_{f\ \mathrm{skin}} + d\eta_{rad} \tag{6}$$

where R_f = average fidelity index for all 99 colour samples; R_{fmin} = value of the lowest-scoring individual R_f (single colour sample); R_{fskin} = average index for two individual colours selected as representative of human skin; η_{rad} = value of LER in lm/W; a, b, c, d are the respective weighting factors.

For the purposes of optimisation, each laser was simulated by a pseudo-delta function (1-nm bandwidth) at the centre wavelength of its output. Optimisations were performed in both constrained (using commercially available laser diode wavelengths) and unconstrained modes.

The best result (with four real laser wavelengths) was R_f of 84 with LER 364 lm/W, which indicates the feasibility of the mixed-laser approach to provide highly efficient, energy-saving light sources. The unconstrained mixtures showed that the prospects will be further enhanced by potential future developments in semiconductor lasers, with the possibility of producing R_f of 86 with LER of 380 lm/W. The detailed properties for these two mixtures are given in **Table 6**.

Compared with LEDs, lasers have the advantage of higher conversion efficiency (from electrical input to radiant output). This, combined with the very high prospective LER values, will make future laser mixtures exceptionally attractive in terms of energy conservation. The colour properties are not as good as for LEDs, but they are nevertheless regarded as sufficiently good for many types of lighting

Simulation mode	R_f	$R_{f\ skin}$	$R_{f\ min}$	i_{min}	LER (lm/W)	CCT (K)
Constrained	84	87	59	97	364	3011
Unconstrained	86	91	54	81	380	3156

i_{min} refers to the sample number that gave the listed value of $R_{f\ i} = R_{f\ min}$,
i = 97 is dark pink-purple (printed origin); 81 is dark purple-blue (natural origin).

Table 6.
Optimizations of simulated tetrachromatic laser mixtures.

situations. Lasers are not yet considered to be practical as white-light sources but, with the potential for new developments in solid-state visible laser sources, their future prospects must be very strong.

5. Conclusions

We have here demonstrated the power of the differential evolution algorithm in the intelligent design of light source spectra, based on both LEDs and laser diodes. It provides a simple, flexible and effective solution in the elusive search for the balance of the LER and the colour rendition properties in optimised light sources. We recommend this technique to anyone engaged in the optimum design of light-source spectra.

We feel confident that our method can also be readily adapted to other types of optimisation problem, wherever suitable elements for the fitness function can be readily identified.

Acknowledgements

This work was supported by Professional Engineering and the Manukau Institute of Technology Research Fund. The second author thanks Professor Ahmed Al-Jumaily, director of IBTec at AUT, for his support and the provision of facilities.

Conflicts of interest

The authors declare that there is no conflict of interest regarding the publication of this chapter.

Funding statement

This study has been supported in part by a Manukau Institute of Technology Research Grant, and was also performed as part of the employment of the authors by Manukau Institute of Technology.

Data availability

Previously reported data were used to support this study. These prior studies are cited at relevant places within the text as references [23, 26–29, 32].

DOI: http://dx.doi.org/10.5772/intechopen.88094

Author details

Snjezana Soltic[1*] and Andrew N. Chalmers[2]

1 Manukau Institute of Technology, Auckland, New Zealand

2 Institute of Biomedical Technologies, Auckland University of Technology, Auckland, New Zealand

*Address all correspondence to: ssoltic@manukau.ac.nz

References

[1] Lei Z, Xia G, Ting L, Xiaoling G, Ming LQ, Guangdi S. Color rendering and luminous efficacy of trichromatic and tetrachromatic LED-based white LEDs. Microelectronics Journal. 2007; **38**:1-6

[2] Stevenson R. The LED's dark secret. IEEE Spectrum. August 2009:23-27

[3] Bergh A, Craford G, Duggal A, Haitz R. The promise and challenge of solid-state lighting. Physics Today. 2001; **54**(12):42-47

[4] Ohno Y. Simulation analysis of white LED spectra and color rendering. CIE Expert Symposium on LED Light Sources, Tokyo; 2004

[5] Žakauskas A, Vaicekauskas R, Ivanauskas F, Gaska R, Shur S. Optimization of white polychromatic semiconductor lamps. Applied Physics Letters. 2002;**80**(2):234-236

[6] Protzman JB, Houser KW. LEDs for general illumination: The state of the science. Leucos. 2006;**3**(2):121-142

[7] Chalmers AN, Cuttle C, Wang L, Luong P. The quest for high-rendering high-luminous-efficacy light sources. In: IESANZ Convention; Queenstown, New Zealand. 2008

[8] Lu Y, Gao Y, Chen H, Chen Z. Intelligent spectra design and colorimetric parameter analysis for light-emitting diodes. In: 14th International Conference on Mechatronics and Machine Vision in Practice, M2VIP 2007, 4-6 Dec. 2007. pp. 118-122

[9] Storn R, Price K. Differential evolution: A simple and efficient adaptive scheme for global optimization over continuous spaces. In: Technical Report TR-95-012. Berkley: International Computer Science Institute; 1995

[10] Storn R, Price K. Differential evolution: A simple and efficient heuristic for global optimization over continuous space. Journal of Global Optimization. 1997;**11**:341-359

[11] Karaboğa D, Ökdem S. A simple and global optimization algorithm for engineering problems: Differential evolution algorithm. Turkey Journal of Electrical Engineering. 2004;**12**(1): 53-60

[12] Vesterstrøm J, Thomsen R. A comparative study of differential evolution, particle swarm optimization, and evolutionary algorithms on numerical bench problems. In: Congress on Evolutionary Computation, 19–23 June; vol. 2. 2004. pp. 1980-1987

[13] CIE. Method of Measuring and Specifying Colour Rendering Properties of Light Sources. Vienna: CIE Publication 13.3, CIE; 1995

[14] Fumagalli S, Bonanomi C, Rizzi A. Experimental assessment of color-rendering indices and color appearance under varying setups. Journal of Modern Optics. 2015;**62**(1):56-66

[15] Illuminating Engineering Society of North America. IES Method for Evaluating Light Source Color Rendition. New York: Illuminating Engineering Society; 2015

[16] David A, Fini PT, Houser KW, Ohno Y, Royer MP, Smet KAG, et al. Development of the IES method for evaluating the color rendition of light sources. Optics Express. 2015;**23**(12): 15888-15906

[17] Royer MP, Wei M. The role of presented objects in deriving color

preference criteria from psychophysical studies. LEUKOS. 2017;**13**(3):143-157

[18] Smet KAG, David A, Whitehead L. Why color space uniformity and sample set spectral uniformity are essential for color rendering measures. LEUKOS. 2016;**12**(1–2):39-50

[19] Luo MR, Cui G, Li C. Uniform colour spaces based on CIECAM02 colour appearance model. Color Research and Application. 2006;**31**: 320-330

[20] CIE. A Colour Appearance Model for Colour Management Systems: CIECAM02. Vienna: CIE Publication 159, CIE; 2004

[21] Davis W, Ohno Y. Color quality scale. Optical Engineering. 2010;**49**(3): 033602

[22] Fairchild MD. Color Appearance Models. 3rd ed. New York: Wiley; 2013

[23] Soltic S, Chalmers AN. Differential evolution for the optimisation of multi-band white LED light sources. Lighting Research and Technology. 2012;**44**(2): 224-237

[24] Wyszecki G, Stiles WS. Color Science: Concepts and Methods, Quantitative Data and Formulae. 2nd ed. New York: Wiley; 1982

[25] Commission Internationale de l'Eclairage. Colorimetry. 3rd ed. Vienna: CIE Publication 15.3, CIE; 2003

[26] Soltic S, Chalmers AN. Differential evolution and its application to intelligent spectral design. In: Proceedings of the 16th Electronics New Zealand Conference (ENZCon); Dunedin: University of Otago. 2009

[27] Chalmers AN, Soltic S. Light source optimization: Spectral design and simulation of four-band white-light sources. Optical Engineering. 2012; **51**(4):044003

[28] Soltic S, Chalmers AN. Optimization of laser-based white light illuminants. Optics Express. 2013;**21**(7):8964-8971

[29] Soltic S, Chalmers AN. Optimization of multiband white-light illuminants for specified color temperatures. Advances in OptoElectronics. 2015. DOI: 10.1155/2015/263791. Article ID: 263791

[30] Lighting L. Luxeon® K2 Emitter, Technical Datasheet DS51. San Jose, California: Lumileds Lighting US LLC; 2006

[31] CIE. Improvement to Industrial Colour-difference Evaluation. Vienna: CIE Publication. 142, CIE; 2001

[32] Soltic S, Chalmers AN. Prospects for 4-Laser white-light sources. Journal of Modern Optics. 2018;**66**(3):271-280. DOI: 10.1080/09500340.2018.1517904

[33] Neumann A, Wierer JJ Jr, Davis W, Ohno Y, Brueck SRJ, Tsao JY. Four-color laser white illuminant demonstrating high color-rendering quality. Optics Express. 2011;**19**(S4 Suppl 4):A982-A990